

The Dielectric Properties of Wood V,* On the Dielectric Anisotropy of Wood.**

Misato NORIMOTO*** and Tadashi YAMADA***

Abstract—This paper deals with the dielectric anisotropy of wood in relation to the structures of wood and the mechanism of the relaxation process due to the motion of CH₂OH group in the disordered region of wood substance.

In very high frequency range in which only optical and infra-red polarizations contribute to dielectric constant, the value of dielectric constant of wood substance in parallel to grain direction was equal to that in perpendicular to grain direction. The dielectric anisotropy of wood, therefore, is mainly caused by the macroscopic structures. On the other hand, in the frequency range in which the relaxation process due to the motion of dipole contributes to dielectric constant, the value of dielectric constant of wood substance in parallel to grain direction was always greater than that in perpendicular to grain direction, and the frequency corresponding to dielectric loss factor maximum in parallel to grain direction was lower than that in perpendicular to grain direction. These results show that the transition probability of dipole jump to an adjacent site when the electric field applies to longitudinal direction is greater than that when the electric field applies to the other directions, and the heights of potential barriers among sites in longitudinal direction are higher than those in the other directions. The dielectric anisotropy of wood in low frequency range, therefore, depends not only upon the macroscopic structures but also upon the molecular structures and motions in wood substance.

Introduction

There are a few reports which deal with the dielectric anisotropy of wood. For instance, KRÖNER reported that the dielectric anisotropy was mainly caused by the macroscopic structure of wood as a mixture of wood substance and air¹⁾. NAKATO and UYEMURA also concluded that the anisotropy of the dielectric constant in the perpendicular to grain direction could be explained by the arrangement of wood cells^{2,3)}. On the other hand, SKAAR reported that the reason for the difference between the parallel to grain and the perpendicular to grain dielectric constants of wood might be resident in ultimate structure of the cell wall⁴⁾.

Up to this time, the dielectric anisotropy of wood has been discussed on the value of dielectric constant at fixed frequency. The problem on the dielectric anisotropy of wood, however, should be considered in connection with dielectric relaxation processes, since it seems that the dielectric anisotropy depends not only

* Previous Paper, Wood Research, No. 50, 36 (1970).

** Presented at the 21th Meeting of Japan Wood Research Society, Nagoya, April 1971.

*** Division of Wood Physics.

upon the macroscopic structures of wood but also upon the molecular structures of wood substance.

In this paper, the dielectric anisotropy of wood is discussed in relation to the macroscopic structures of wood and the motions of dipoles in wood substance.

Experimental

The wood specimens used are shown in Table 1. Before the measurement the specimens were dried at 105°C and then were dried over the phosphorus pentoxide *in vacuo* (10^{-3} mmHg) at room temperature. The all measurements were performed at the absolutely dried condition.

Table 1. Wood specimens.

Species	Specific gravity	Direction	Thickness (mm)	Treatment
Hoonoki (<i>Magnolia obovata</i> THUNB.)	0.48 0.45	L, R, T	1.9, 1.5 5.0	untreated, hot water and alcohol- benzene extraction
Keyaki (<i>Zelkova serrata</i> MAKINO)	0.65	L, T	1.2	hot water and alcohol- benzene extraction
Western hemlock (<i>Thuja heterophylla</i> SARGENT)	0.48	L, R, T	1.3	untreated
Kiri (<i>Paulownia tomentosa</i> STEUD.)	0.30	L, R, T	1.4	untreated
Makanba (<i>Betura maximowicziana</i> REGEL)	0.61	L, R, T	1.5	untreated
Kashi (<i>Quercus</i> spp.)	0.81	L, R, T	1.5	untreated

The inductive ratio arm bridge was used for the measurement of the dielectric properties of wood in the frequency range from 30 Hz to 1 MHz and in the temperature range from -60° to 20° C.

Results and Discussion

The dielectric dispersion and absorption curves for Hoonoki in L direction (longitudinal direction) at respective temperatures are shown in Figs. 1 and 2. The corresponding curves for Keyaki in L and T (tangential direction) directions are shown in Figs. 3 and 4. A relaxation process was observed in the frequency range at low temperature. The value of dielectric constant decreased with increasing

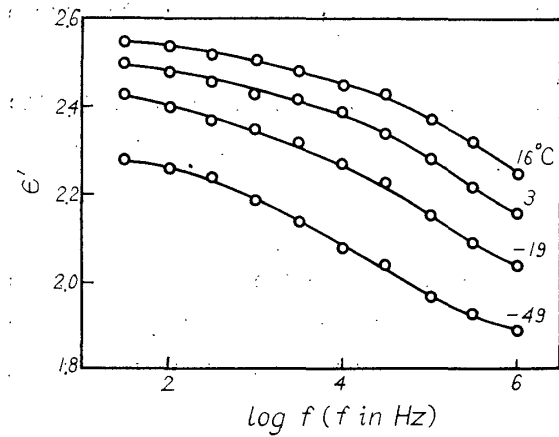


Fig. 1. The dielectric dispersion curves for Hoonoki in L direction at respective temperatures.

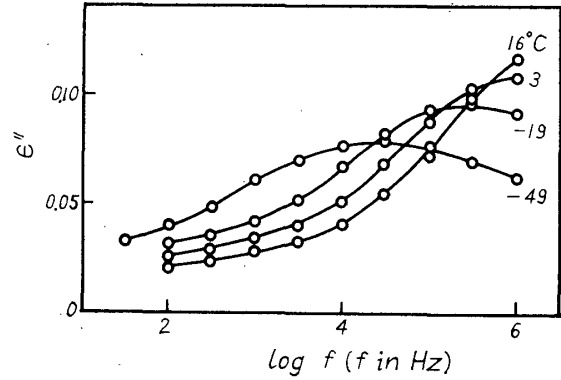


Fig. 2. The dielectric absorption curves for Hoonoki in L direction at respective temperatures.

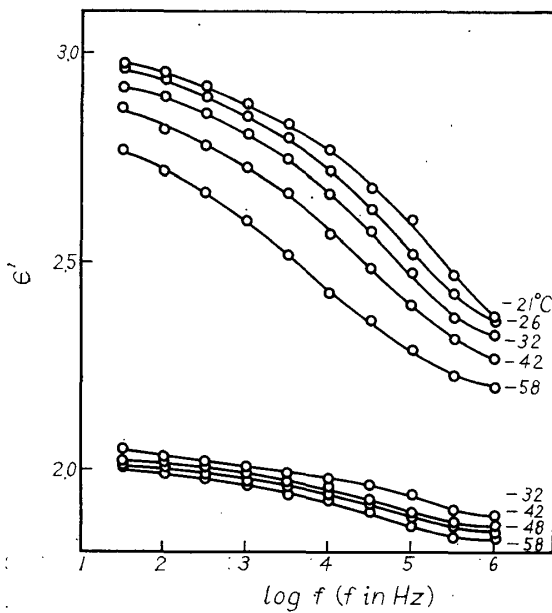


Fig. 3. The dielectric dispersion curves for Keyaki in L (upper curves) and T (lower curves) directions at respective temperatures.

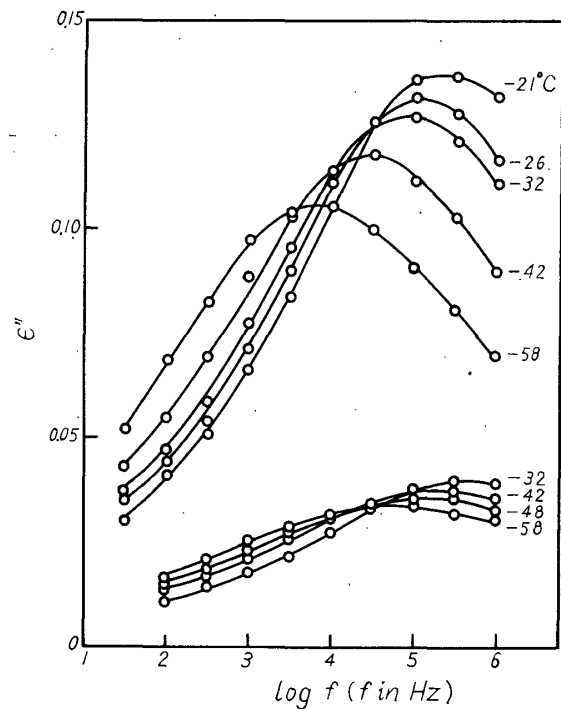


Fig. 4. The dielectric absorption curves for Keyaki in L (upper curves) and T (lower curves) directions at respective temperatures.

frequency and with decreasing temperature. The maximum value of dielectric loss factor decreased with decreasing temperature and the frequency corresponding to the dielectric loss factor maximum shifted to the low frequency range with decreasing temperature. It has already been explained in the previous paper⁵⁾ that the dispersion is due to the motion of CH_2OH group in disordered region of wood

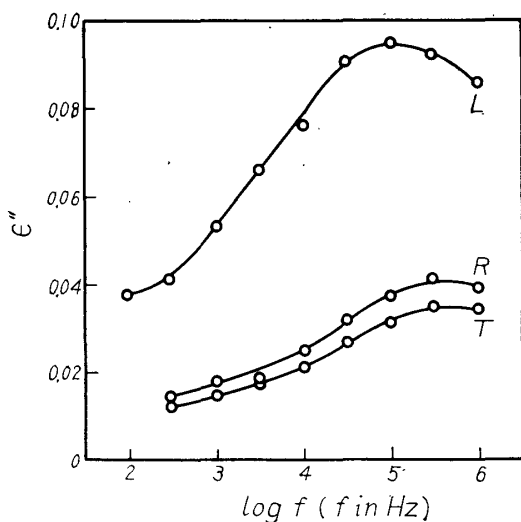


Fig. 5. The dielectric loss factor vs. frequency curves for Hoonoki in L, R and T directions at -32°C .

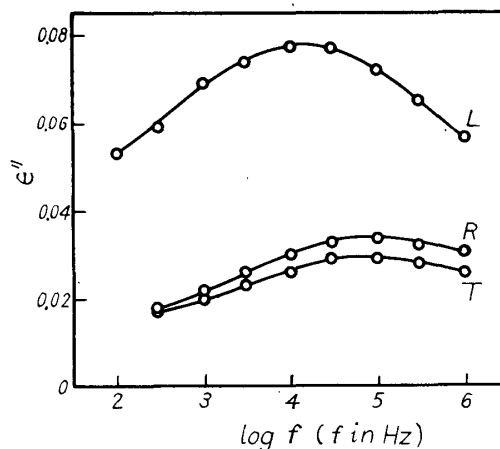


Fig. 6. The dielectric loss factor vs. frequency curves for Hoonoki in L, R and T directions at -58°C .

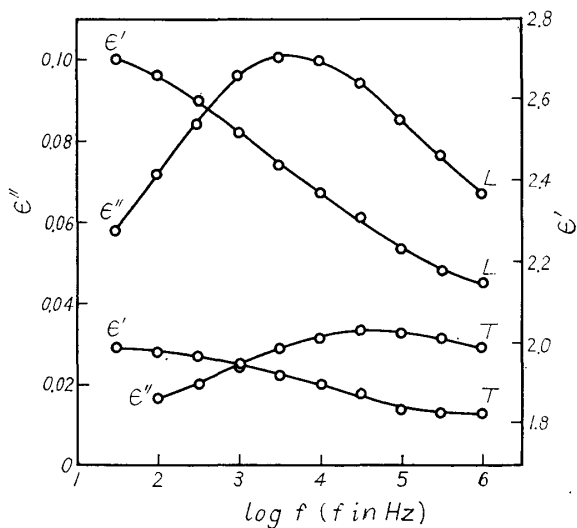


Fig. 7. The dielectric constant and the dielectric loss factor vs. frequency curves for Keyaki in L and T directions at -58°C .

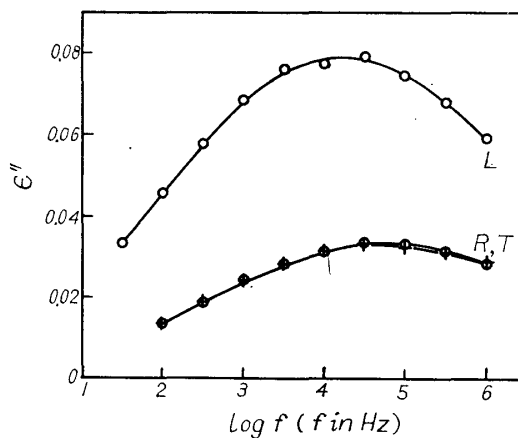
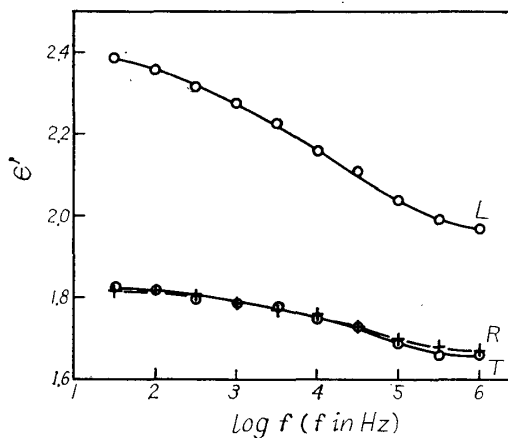


Fig. 8. The dielectric dispersion and absorption curves for western hemlock in L, R and T directions at -58°C .

substance. The dielectric loss factor ϵ'' as a function of frequency for Hoonoki in the three principal directions at -32° and -58°C are shown in Figs. 5 and 6. The dielectric constant ϵ' and the dielectric loss factor ϵ'' as a function of frequency for Keyaki in L and T directions at -58°C are shown in Fig. 7. The corresponding curves for western hemlock in the three principal directions are shown in Fig. 8. The value of ϵ'' for Hoonoki decreased in the order, L direction > R direction > T direction. On the other hand, the values of ϵ' and ϵ'' in L direction for western hemlock were greater than those in the other directions, while there was no difference between the values in the transverse directions. The frequency corresponding to the ϵ'' maximum in L direction existed in the lower frequency range than those in the other directions. Table 2 shows the value of ϵ' for a few wood species in the three principal directions. As is evident from the table, the value of ϵ' in L direction was always greater than those in the other directions, and for Hoonoki the value in R direction (radial direction) was greater than that in T direction,

Table 2. The values of ϵ' for a few wood species at oven dried condition.

Species	Direction	Freq. (Hz)	Temp. ($^\circ\text{C}$)	ϵ'	
Kiri	L	10^6	20	1.85	
	R			1.40	
	T			1.51	
Hoonoki	L			2.49	
	R			1.91	
	T			1.77	
Makanba	L			2.71	
	R			2.03	
	T			2.01	
Kashi	L	30	-58	3.08	
	R			2.31	
	T			2.40	
	L			2.51	
	R			2.09	
	T			2.16	
western hemlock	L	10^6	-58	1.97	
	R			1.67	
	T			1.66	
	L			30	2.39
	R				1.82
	T				1.83

while for Kiri and Kashi in R direction was smaller than that in T direction. On the other hand, there was no difference between the values of ϵ' in the transverse directions for Makanba and western hemlock.

1. *The dielectric anisotropy and macroscopic structures of wood*

LICHTENECKER and ROTHER gave the following equation for the dielectric constant of a mixture.⁶⁾

$$\epsilon'^k = \delta_1 \epsilon_1'^k + \delta_2 \epsilon_2'^k, \quad -1 \leq k \leq 1 \quad (1)$$

where ϵ' , ϵ_1' and ϵ_2' are the dielectric constants of the mixture and the components 1 and 2, and δ_1 and δ_2 are the volume fractions of the components, respectively. WIENER showed the following equations for the dielectric constants of a lamellar mixture.⁷⁾

$$\frac{1}{\epsilon_{\perp}'} = \frac{\delta_1}{\epsilon_1'} + \frac{\delta_2}{\epsilon_2'} \quad (2)$$

$$\epsilon_{\parallel}' = \delta_1 \epsilon_1' + \delta_2 \epsilon_2' \quad (3)$$

where ϵ_{\perp}' and ϵ_{\parallel}' are the dielectric constants perpendicular and parallel to the lamellae, respectively. The equations (2) and (3) are equivalent to the cases of $k = -1$ and $k = 1$ in the equation (1), respectively. KRÖNER et al. represented the perpendicular and the parallel to grain dielectric constants by the equations (2) and (3) respectively, and gave the following equation for the dielectric constant of cell wall.¹⁾

$$\epsilon_1' = \frac{1}{2(\epsilon_{\parallel}' - 1)} [(\epsilon_L' \epsilon_{\parallel}' - 1) + \sqrt{(\epsilon_L' \epsilon_{\parallel}' - 1)^2 - 4(\epsilon_L' - 1)(\epsilon_{\parallel}' - 1)}] \quad (4)$$

where ϵ_L' and ϵ_{\parallel}' are the dielectric constants in L and T directions. The value of dielectric constant of cell wall calculated by them was 4.40 for Fichte at 300 Hz. They also showed the relation between the dielectric constants of cell wall and wood substance.

$$\log \epsilon_1' = \delta_w \log \epsilon_w' \quad (5)$$

where δ_w and ϵ_w' are the volume fraction of wood substance in cell wall and the dielectric constant of wood substance.

NAKATO gave the following equation for ϵ_{\perp}' in due consideration of the actual macroscopic structures of wood.²⁾

$$\epsilon_{\perp}' = \epsilon_1' \delta_1 \theta_2 + \frac{\epsilon_1' (1 - \delta_1 \theta_2)^2}{\epsilon_1' (1 - \delta_1) + \delta_1 \theta_1} \quad (6)$$

where θ_1 and θ_2 are the volume fractions of cell wall in series and parallel with cell lumen, respectively. UYEMURA introduced the equation for ϵ_{\perp}' from the equations (2) and (3).³⁾

$$\epsilon'_{R \text{ or } T} = K_{R \text{ or } T} \left[1 + \frac{\gamma}{\gamma_1} (\epsilon'_1 - 1) \right] + \frac{(1 - K_{R \text{ or } T}) \epsilon'_1}{\epsilon'_1 - \frac{\gamma}{\gamma_1} (\epsilon'_1 - 1)} \quad (7)$$

$$K_R + K_T = 1$$

where γ and γ_1 are the specific gravities of wood and wood cell wall, and K is the constant representing the anisotropy.

Fig. 9 shows the relation between the dielectric constants in parallel and perpendicular to grain at 1 MHz and 20°C and the specific gravity of wood γ . In this figure the results reported by UYEMURA,³⁾ NAKATO,²⁾ TAKEMURA,⁸⁾ and SUZUKI⁹⁾ are included. Our results agreed well with their results, especially with UYEMURA's results. In the figure the solid lines represent the values calculated by the equations (3) and (7), and the calculated values agreed well with the experimental ones. The values of dielectric constant parallel and perpendicular to grain at $\gamma = 1.43$, which represents the density not only of wood cell wall but also of the wood substance,¹⁰⁾ calculated from the equations (3) and (7) were 5.0 and 4.3, respec-

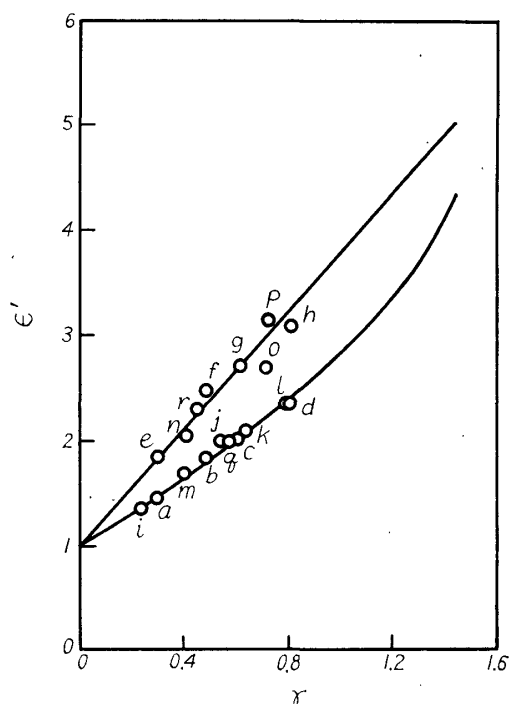


Fig. 9. The relationship between dielectric constant and specific gravity. *a*, Kiri (ϵ'_{\perp}). *b*, Hoonoki (ϵ'_{\perp}). *c*, Mankanba (ϵ'_{\perp}). *d*, Kashi (ϵ'_{\perp}). *e*, Kiri (ϵ'_{\parallel}). *f*, Hoonoki (ϵ'_{\parallel}). *g*, Mankanba (ϵ'_{\parallel}). *h*, Kashi (ϵ'_{\parallel}). *i*, Kiri (ϵ'_{\perp} , T. UYEMURA³⁾). *j*, Hoonoki (ϵ'_{\perp} , T. UYEMURA). *k*, Mankanba (ϵ'_{\perp} , T. UYEMURA). *l*, Kashi (ϵ'_{\perp} , T. UYEMURA). *m*, Hinoki (ϵ'_{\perp} , calculated value, K. NAKATO²⁾). *n*, Hinoki (ϵ'_{\parallel} , calculated value, K. NAKATO). *o*, Mizunara (ϵ'_{\perp} , calculated value, K. NAKATO). *p*, Mizunara (ϵ'_{\parallel} , calculated value, K. NAKATO). *q*, Buna (ϵ'_{R} , T. TAKEMURA⁸⁾). *r*, Hinoki (ϵ'_{\parallel} , M. SUZUKI⁹⁾).

Table 3. The dielectric constant of cell wall and wood substance.

Species	f (Hz)	T (°)	dielectric constant of cell wall or wood substance	Reference
Fichte Buche	3×10^2 5×10^2	20	4.40 4.70 (cell wall)	KRÖNER et al. ¹⁾
		20	9.4 (L) 8.3 (R) (wood substance)	KRÖNER et al. ¹⁾
Fichte	1×10^3	20	6.6 (T) (wood substance)	TRAPP et al. ³³⁾
Rotbuche	1×10^6		3.9 (R, T) (specific gravity = 1.40)	RAFALSKI ³²⁾
30 wood species	2×10^6		4.2 (\perp) (wood substance)	SKAAR ⁴⁾
Hinoki	0.55×10^6 1.90×10^6	30	3.67 (\perp) 3.25 (\perp) (cell wall)	NAKATO et al. ²⁾
many wood species	1×10^6	20	4.8 (\perp) (wood substance)	UYEMURA ³⁾
many wood species	1×10^6	20	5.0 (L) 4.4 (\perp) (cell wall)	NORIMOTO and YAMADA

tively. For comparison, the values of dielectric constant for wood cell wall and wood substance reported by many investigators are shown in Table 3. Under the condition at 1 MHz and 20°C, the greater part of relaxation process, which is due to the motion of CH₂OH group in the amorphous region of wood substance as reported in the previous paper,⁵⁾ contributes to the dielectric constant. In Fig. 10 the dielectric constants of wood (western hemlock) and wood substance in parallel and perpendicular to grain at -58°C as a function of frequency are shown. The

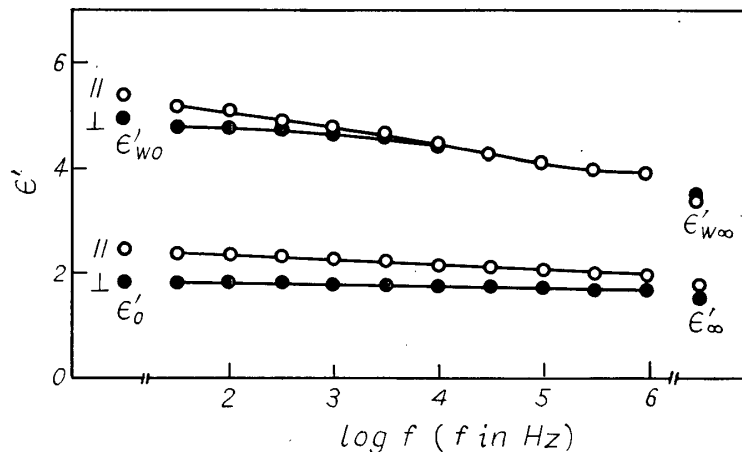


Fig. 10. The dielectric constants of western hemlock and wood substance in parallel and perpendicular to grain at -58°C as a function of frequency.

values of ϵ_0' and ϵ_∞' in the figure were calculated from COLE-COLE'S plots. The value of $\epsilon'_{w\infty}$ in parallel to grain was identical with that in perpendicular to grain. In other words, the dielectric anisotropy of wood is caused by the macroscopic structures in very high frequency range in which only optical and infra-red polarizations contribute to dielectric constant. On the other hand, the value of ϵ_w' in parallel to grain was slightly greater than that in perpendicular to grain in low frequency range. These results show that the dielectric anisotropy depends not only upon the macroscopic structures but also upon the molecular structures in wood substance in the frequency range in which the orientational polarization contributes to dielectric constant. The reason for the dielectric anisotropy in wood substance will be discussed later.

2. *The application of Cole-Cole's circular arc law to the dielectric properties of wood.*

The complex dielectric constant ϵ^* for a number of dielectrics is represented by the following COLE-COLE'S circular arc law.¹¹⁾

$$\epsilon^* - \epsilon_\infty' = \frac{\epsilon_0' - \epsilon_\infty'}{1 + (i\omega\tau_0)^{1-\alpha}} \quad (8)$$

where ϵ_0' and ϵ_∞' are the static and the infinite frequency dielectric constants, and τ_0 and α ($0 \leq \alpha \leq 1$) are the generalized relaxation time and the parameter relating to the distribution of relaxation times. The locus of the equation (8) in complex plane shows a circular arc. Although the width of the distribution of relaxation times can be estimated quantitatively from COLE-COLE'S circular arc law, it is difficult to understand the physical significance of the equation. HIGASI et al. reported about the relation between COLE-COLE'S circular arc law and the function for the distribution of relaxation times similar to that derived by FRÖHLICH, and explained qualitatively the physical picture of COLE-COLE'S equation.^{12,13)}

For the first time TAKEDA showed that COLE-COLE'S arc law could be applied to the dielectric relaxation process of wood.¹⁴⁾ Tsutsumi showed that the dielectric dispersions of wood in L direction in both lower and higher frequency regions satisfied COLE-COLE'S law, and with increase in temperature the value of $(\epsilon_0' - \epsilon_\infty')$ decreased and in contrast with this the value of α increased.¹⁵⁾ Recently, NANASSY applied the law to the experimental results of oven dried yellow birch.¹⁶⁾ ISHIDA et al. applied the law to the various cellulose fibers in the direction of fiber axis, and showed that the dipoles in the amorphous region and surface of crystallites could make a great contribution to the dielectric dispersion, since the value of $(\epsilon_0' - \epsilon_\infty')$ for dry cellulose fibers decreased with increase in degree of crystallinity.¹⁷⁾

The results of COLE-COLE'S plots for Hoonoki, Keyaki and western hemlock

are shown in Figs. 11, 12 and 13, respectively. The experimental values agreed well with the equation (8). The values of $(\epsilon_0' - \epsilon_\infty')$ and $\frac{\pi}{2} \cdot \alpha$ at various conditions of temperature and frequency for four wood species are shown in Table 4. The width of the distribution of relaxation times became narrow with increasing temperature. The value of $(\epsilon_0' - \epsilon_\infty')$ in L direction was always higher than that in transverse directions, while there was no difference among the widths of the distribution of relaxation times in three directions. The result of temperature dependence of $(1-\alpha)$ for wood in L direction is shown in Fig. 14 and compared with those obtained by TSUTSUMI and NANASSY for wood and by ISHIDA et al. for Bemberg. Our

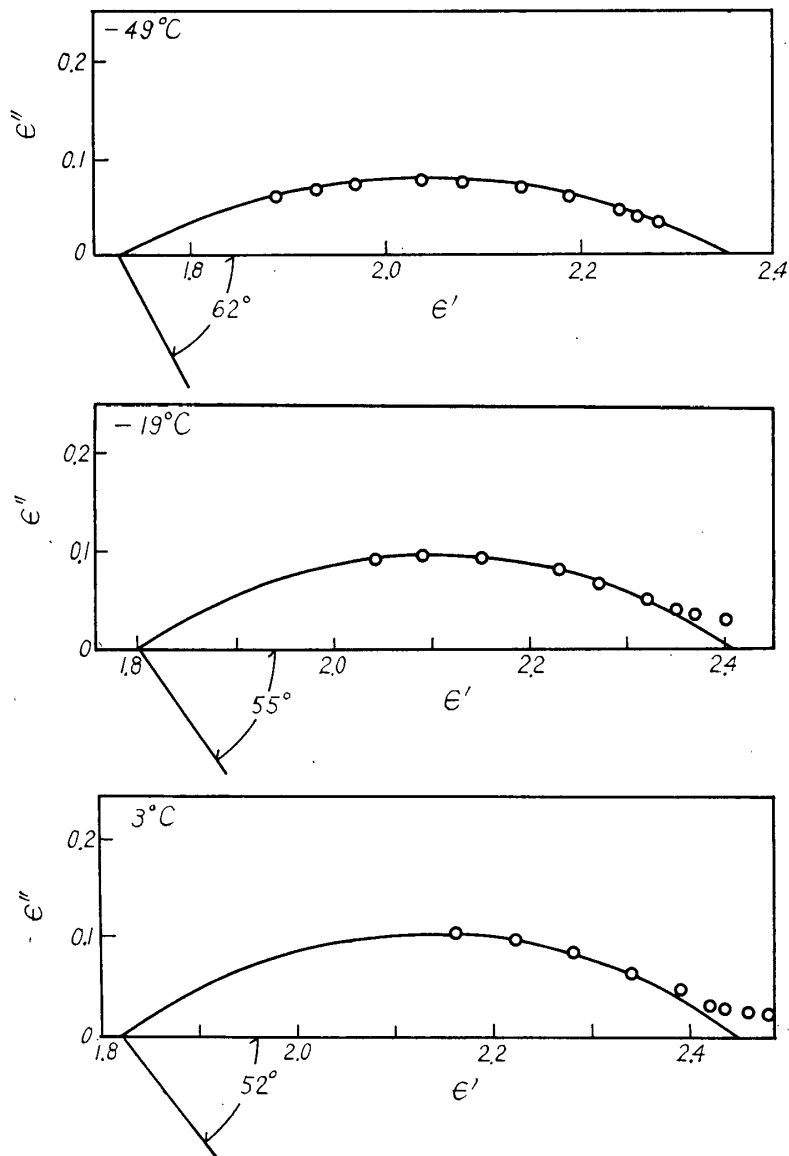


Fig. 11. The COLE-COLE'S plots for Hoonoki in L direction at -49° , -19° and 3°C .

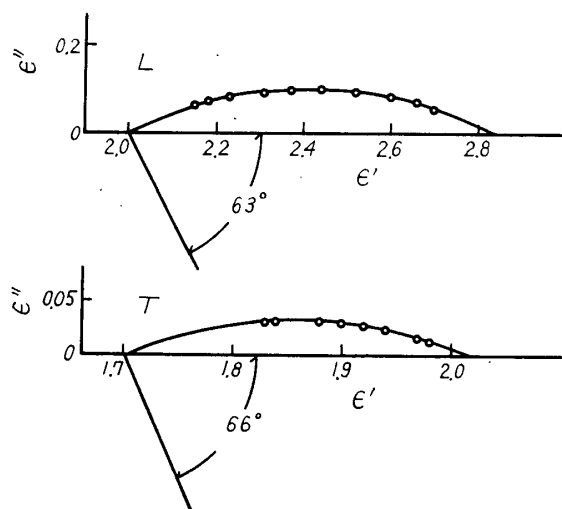


Fig. 12. The COLE-COLE'S plots for Keyaki in L and T directions at -58°C .

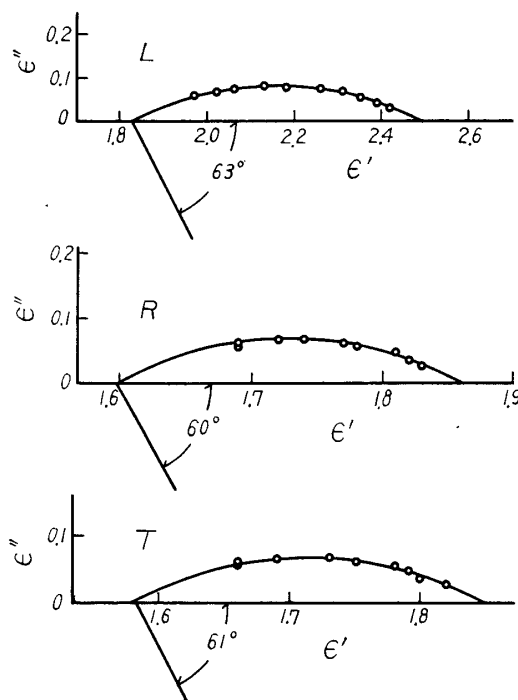


Fig. 13. The COLE-COLE'S plots for western hemlock in L, R and T directions at -58°C .

Table 4. The values of $(\epsilon_0' - \epsilon_{\infty}')$ and parameter $\frac{\pi}{2} \cdot \alpha$ calculated from COLE-COLE'S plot for four wood species.

Species	Direction	Temp. ($^{\circ}\text{C}$)	$\epsilon_0' - \epsilon_{\infty}'$	$\frac{\pi}{2} \cdot \alpha$ ($^{\circ}$)
Hoonoki	L	3	0.63	52
		-19	0.61	55
		-49	0.63	62
Keyaki	L	-58	0.84	63
	T		0.33	66
western hemlock	L		0.66	64
	R		0.26	61
	T		0.27	61
Kashi	L		0.83	64
	R	0.37	65	
	T	0.32	64	

result agreed well with ISHIDA'S result for cellulose fiber.

3. The application of Hoffman's theory to the dielectric relaxation process of wood.

MIKHAILOV et al. investigated the dielectric relaxation in the glass-like state of

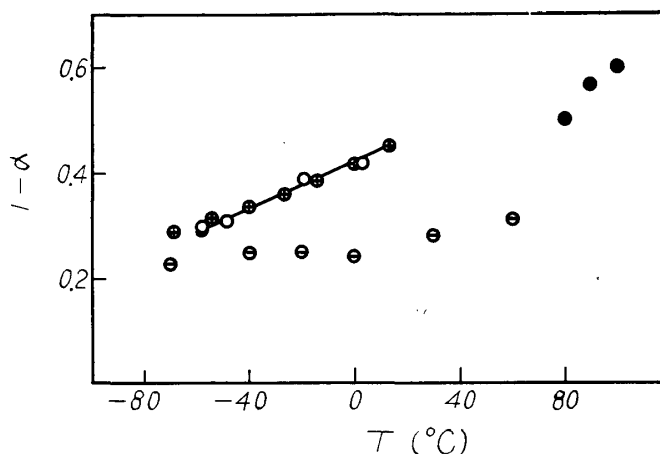


Fig. 14. The relationship between the parameter $(1-\alpha)$ and temperature for wood and cellulose.

○: Hoonoki in L direction, ⊙: TSUTSUMI'S result for Buna in L direction¹⁵⁾, ●: NANASSY'S result in L direction¹⁶⁾, ⊕: ISHIDA'S result for cellulose fiber¹⁷⁾.

cellulose and its derivatives, and explained that the relaxation might be due to the movement of CH_2OH group in the less ordered zones of the polymer from the results of NMR study.¹⁸⁾ In the previous paper, we reported that the dielectric dispersion of oven dried wood and cellulose in high frequency region might be caused by the movement of CH_2OH group since the dispersion did not occur in beech xylan, which has not CH_2OH group.⁵⁾

Fig. 15 shows the mode of molecular motion of a primary hydroxyl group in a glucose unit. ZHBANKOV reported that O_6 atom in CH_2OH group has three stable positions, namely at 80° , 177° and 300° clockwise from the cis-position of the O_6 and C_4 atoms. The calculated value of the energy barrier among the sites was $3\sim 10$ kcal/mole and was almost equivalent to the apparent energy of activation calculated from the curve of the frequency corresponding to the dielectric loss factor maximum versus the reciprocal of absolute temperature.^{20,21)} As a simple case,

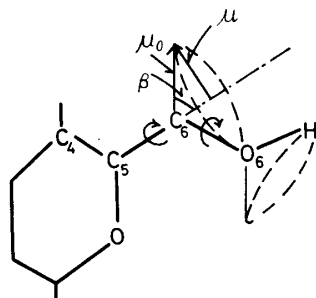


Fig. 15. The mode of molecular motion of a primary hydroxyl group in a glucose unit.

let us consider a model in which O_6 atom has two stable positions 180° apart, namely 120° and 300° , since the energy barrier between 80° and 177° is remarkably low compared with the others. The theory associated with so called site models have been treated by DEBYE,²²⁾ KAUZMANN,²³⁾ FRÖHLICH,²⁴⁾ HOFFMAN,²⁵⁾ and ISHIDA and YAMAFUJI.²⁶⁾ In this paper, HOFFMAN'S two position model is used to account for the dielectric dispersion of wood.

The coordinate system used in the calculation of the complex dielectric constant is shown in Fig. 16. O_6 atom can rotate on XY plane and the stable positions of the atom 180° apart are fixed on the X axis. The electric field F applies to the direction having the polar angle θ and the longitude φ with respect to the coordinate. By generalization of the theory on HOFFMAN'S two positions model, the total polarization P is given by

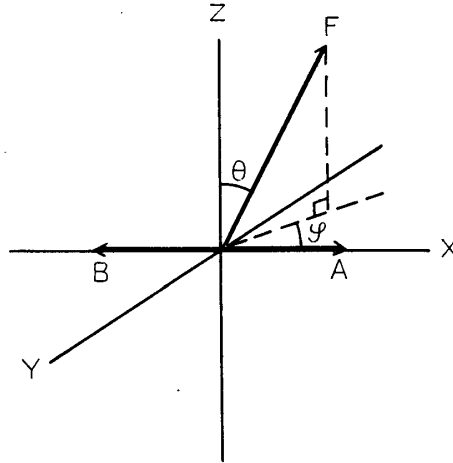


Fig. 16. The coordinate system used in the calculation of the complex dielectric constant of wood.

$$\begin{aligned}
 P &= \langle \sum_i P_i \rangle_{AV} = \sum_i \frac{4N_{iA}N_{iB}\mu F}{N_i kT} \int_{\varphi=0}^{2\pi} \int_{\theta=0}^{\pi} \frac{\sin^2\theta \cos^2\varphi \sin\theta \cdot d\theta \cdot d\varphi}{4\pi} \\
 &= \sum_i \frac{1}{3} \cdot \frac{4N_{iA}N_{iB}\mu F}{N_i kT} \quad (9) \\
 N_i &= N_{iA} + N_{iB}, \quad N = \sum N_i \\
 \mu &= \mu_0 \sin \beta
 \end{aligned}$$

where N_{iA} and N_{iB} are number of dipoles in site A and B in i -th energy state, and N is total number of dipoles, k and T are BOLTZMANN'S constant and absolute temperature, μ , μ_0 and β are the component of the permanent dipole moment perpendicular to the axis of rotation, the permanent dipole moment in C_6O_6 direction and the angle subtended by the dipole and the axis of rotation, respectively. Then, the polarizability α and the complex dielectric constant ϵ^* are given by

$$\alpha = \frac{P}{NF} = \sum_i \frac{4\mu N_{iA} N_{iB}}{3kT N_i N} \quad (10)$$

$$\epsilon^* - \epsilon_{\infty}' \approx \sum_i \frac{S4\mu N_{iA} N_{iB}}{3kT N_i N} \cdot \frac{1}{1+i\omega\tau_i} \quad (11)$$

$$\epsilon_0' - \epsilon_{\infty}' \approx S \sum_i \frac{4\mu N_{iA} N_{iB}}{3kT N_i N}$$

where S is the constant. When the relaxation times distribute continuously, ϵ^* is given by the following equation.

$$\begin{aligned} \epsilon^* - \epsilon_{\infty}' &= \int_0^{\infty} (\epsilon_0' - \epsilon_{\infty}') \frac{y(\tau)}{1+i\omega\tau} \cdot d\tau \\ &= \int_{-\infty}^{\infty} (\epsilon_0' - \epsilon_{\infty}') \frac{\Phi(\ln \tau)}{1+i\omega\tau} \cdot d \ln \tau \\ &= \int_{-\infty}^{\infty} (\epsilon_0' - \epsilon_{\infty}') \frac{\bar{\Phi}(\log \tau)}{1+i\omega\tau} \cdot d \log \tau \end{aligned} \quad (12)$$

$$\frac{\epsilon' - \epsilon_{\infty}'}{\epsilon_0' - \epsilon_{\infty}'} = \int_{-\infty}^{\infty} \frac{\bar{\Phi}(\log \tau)}{1+\omega^2\tau^2} \cdot d \log \tau \quad (12-a)$$

$$\frac{\epsilon''}{\epsilon_0' - \epsilon_{\infty}'} = \int_{-\infty}^{\infty} \frac{\bar{\Phi}(\log \tau)\omega\tau}{1+\omega^2\tau^2} \cdot d \log \tau \quad (12-b)$$

$$\int_0^{\infty} y(\tau) d\tau = \int_{-\infty}^{\infty} \Phi(\ln \tau) d \ln \tau = \int_{-\infty}^{\infty} \bar{\Phi}(\log \tau) \cdot d \log \tau = 1$$

where the functions $y(\tau)$, $\Phi(\ln \tau)$ and $\bar{\Phi}(\log \tau)$ are the distribution of relaxation times. The relation among $\bar{\Phi}(\log \tau)$, $\Phi(\ln \tau)$ and $y(\tau)$ is given by

$$\bar{\Phi}(\log \tau) = 2.303 \Phi(\ln \tau) = 2.303 \tau y(\tau) \quad (13)$$

Thus, the general form of DEBYE's equation can be obtained by the generalization of HOFFMAN's theory.

4. The application of Fröhlich's theory to the dielectric properties of wood.

FRÖHLICH proposed the theory of dielectric relaxation on the two position model.²⁴⁾ In his theory, the following points are assumed: (1) the potential barrier between the two positions has a different height for each molecule and the heights of the potential barriers H distribute over a range between H_0 and $H_0 + v_0$, (2) the interaction between dipoles can be neglected and the contribution of a dipolar molecule to ϵ_0' is independent of H , (3) the relaxation time depends on H . The distribution function of relaxation times and dielectric properties, ϵ' and ϵ'' , are given by

$$\begin{aligned} y(\tau) &= \frac{kT}{v_0} \cdot \frac{1}{\tau} \quad (\tau_1 \leq \tau \leq \tau_2) \\ y(\tau) &= 0 \quad (\tau < \tau_1, \tau > \tau_2) \\ \frac{\epsilon' - \epsilon_{\infty}'}{\epsilon_0' - \epsilon_{\infty}'} &= 1 - \frac{kT}{2v_0} \ln \frac{1 + \omega^2\tau_1^2 e^{\frac{2v_0}{kT}}}{1 + \omega^2\tau_1^2} \end{aligned} \quad (14)$$

$$\frac{\epsilon''}{\epsilon_0' - \epsilon_\infty'} = \frac{kT}{v_0} \left[\tan^{-1}(\omega\tau_1 e^{\frac{v_0}{kT}}) - \tan^{-1}\omega\tau_1 \right] \quad (15)$$

where τ_2 and τ_1 are the maximum and the minimum relaxation times, respectively.

HIGASHI et al. discussed the relationship between FRÖHLICH's theory and COLE-COLE's circular arc law¹²⁾ and showed the following relation between the parameter α and $\frac{v_0}{kT}$.

$$\alpha = 1 - \frac{4}{\pi} \tan^{-1} \left[\frac{2kT}{v_0} \tan^{-1} \sinh \frac{v_0}{2kT} \right] \quad (16)$$

$$\tau_1 = \tau_0 e^{-\frac{v_0}{2kT}}, \quad \tau_2 = \tau_0 e^{\frac{v_0}{2kT}}$$

The values of τ_2 , τ_1 and v_0 calculated from the equation (16) for Hoonoki in L direction at -49°C were 2.88×10^{-3} sec, 9.75×10^{-9} sec and 5.60 kcal/mole (3.90×10^{13} erg), respectively. In Fig. 17 the comparison between the calculated and the experimental values of ϵ' and ϵ'' is shown. The FRÖHLICH's theory could not exactly be applied to the results of wood. The relaxation times, therefore, do not distribute uniformly in wood substance.

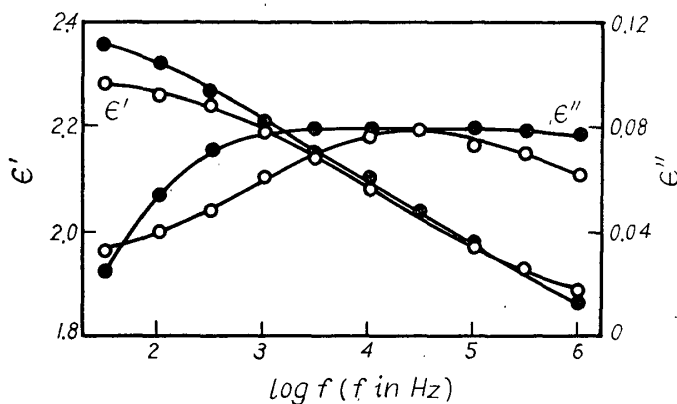


Fig. 17. The dielectric dispersion and absorption curves for Hoonoki.
 ○: experimental, ●: predicted by the barrier theory of FRÖHLICH.

5. The calculation of the distribution of relaxation times of wood.

FUOSS and KIRKWOOD reported that the distribution function of relaxation times could be calculated by the following equation, if ϵ'' could be empirically represented by an analytic function.²⁷⁾

$$\pi\Phi(S) = H\left(S + \frac{i\pi}{2}\right) + H\left(S - \frac{i\pi}{2}\right) \quad (17)$$

$$\Phi(S) = \tau y(\tau), \quad S = \ln \tau / \tau_0$$

$$H(\omega) = \frac{\epsilon''}{\epsilon_0' - \epsilon_\infty'} = \int_0^\infty \frac{y(\tau)\omega\tau}{1 + \omega^2\tau^2} \cdot d\tau \quad (18)$$

They also showed that $H(x)$ for a number of polar polymers could be represented by the empirical equation (19) and obtained the distribution function of relaxation times (20) by the substitution of (19) in (17).

$$H(x) = H(0) \operatorname{sech} Ax, \quad x = \ln \omega_0/\omega \quad (19)$$

$$\frac{\phi(S)}{H(0)} = \frac{2}{\pi} \cdot \frac{\cos(A\pi/2) \cosh AS}{\cos^2(A\pi/2) + \sinh^2 AS} \quad (20)$$

where A is a parameter which measures the width of the distribution of relaxation times, and $H(0)$ is the maximum value of $H(x)$.

The values of $H(0)$ and A are determined by the following equations.

$$H(0) = \frac{A}{2} \quad (21)$$

$$\cosh^{-1} \frac{H(0)}{H(x)} = Ax \quad (22)$$

The value of $(\epsilon'_0 - \epsilon'_\infty)$ calculated from A for Hoonoki was 0.72 and was slightly larger than that obtained by COLE-COLE'S plot. In Fig. 18 $\cosh^{-1} H(0)/H(x)$ vs. $\log \omega_0/\omega$ curve for Hoonoki is shown. The value of A calculated from the slope of the straight line was 0.217. In Fig. 19 the values of ϵ'' for Hoonoki calculated from the following relation are compared with the experimental ones. The experimental values were in satisfactory agreement with the empirical equation.

$$\epsilon'' = \epsilon''_{max} \operatorname{sech} [2.303A(\log f_0/f)] \quad (23)$$

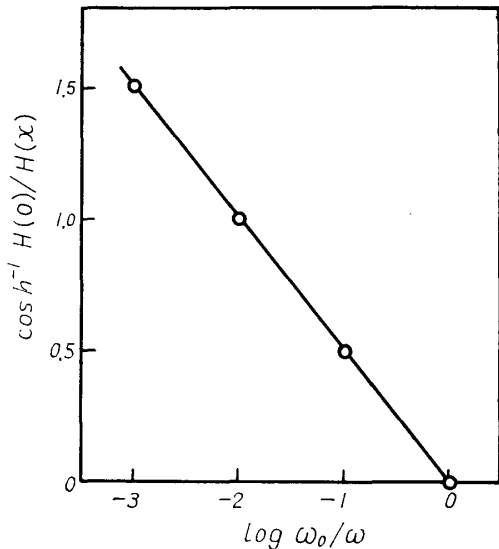


Fig. 18. $\cosh^{-1} H(0)/H(x)$ vs. $\log \omega_0/\omega$ curve for Hoonoki.

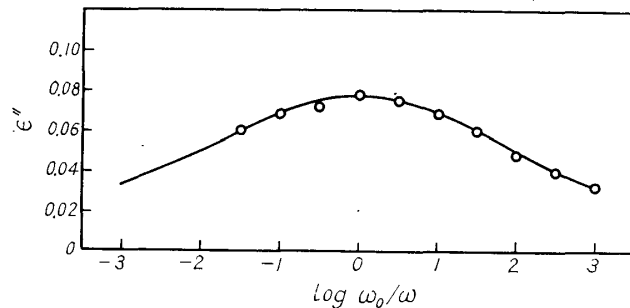


Fig. 19. The dielectric absorption curve for Hoonoki in L direction.

○: experimental, —: calculated (equation (23)).

In Fig. 20 the distribution function of relaxation times for Hoonoki calculated from the equation (20) is shown, together with those obtained by the approximation

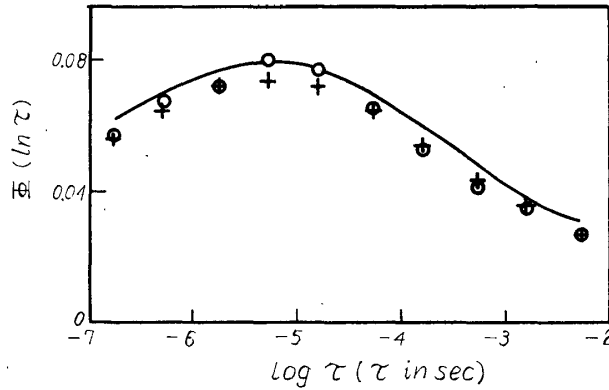


Fig. 20. The distribution function of relaxation times of Hoonoki in L direction.
 —: zero order approximation, ○: second order approximation, +: equation (20).

methods.

On the other hand, the distribution function can be calculated directly from the equations (12-a) and (12-b) by the approximate methods. The zero order and the first order approximations,²⁸⁾ and the second order approximation²⁹⁾ proposed by WILLIAMS and FERRY are given by

$$\Phi_0(\ln \tau) = \frac{2}{\pi} \cdot \frac{\epsilon''}{\epsilon_0' - \epsilon_{\infty}'} \quad (24)$$

$$\Phi_1(\ln \tau) = -\frac{\epsilon' - \epsilon_{\infty}'}{\epsilon_0' - \epsilon_{\infty}'} / d \ln \omega \quad (25)$$

$$\Phi_2(\ln \tau) = B \frac{\epsilon''}{\epsilon_0' - \epsilon_{\infty}'} \left(1 - |d \log \frac{\epsilon''}{\epsilon_0' - \epsilon_{\infty}'} / d \log \omega| \right) \quad (26)$$

$$B = (1 + |m|) / 2 \Gamma\left(\frac{3}{2} - \frac{|m|}{2}\right) \Gamma\left(\frac{3}{2} + \frac{|m|}{2}\right)$$

$$m = \frac{d \log \Phi_1(\ln \tau)}{d \log \tau}$$

where Γ is gamma function.

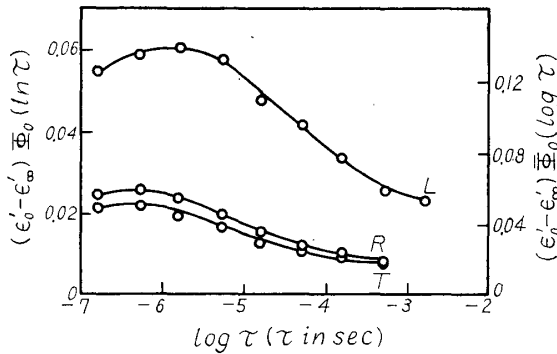


Fig. 21. The distribution function of relaxation times for Hoonoki in L, R and T directions at -32°C .

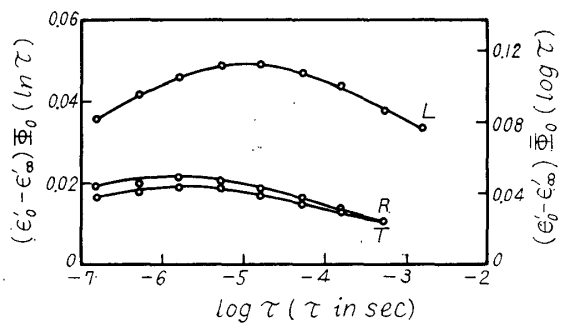


Fig. 22. The distribution function of relaxation times for Hoonoki in L, R and T directions at -58°C .

In Fig. 20 the distribution functions calculated from the equations (24) and (26) are shown together with that obtained by the equation (20). As is evident from the figure, the values calculated from these distribution functions were almost identical. In Figs. 21 and 22 the distribution functions calculated from the equation (24) for Hoonoki at -32° and -58°C are shown.

WAGNER proposed that the distribution function of relaxation times was governed by a probability function in dielectrics,³⁰⁾ and YAGER described the graphical method of evaluating the constants of the following WAGNER's equations for ϵ' and ϵ'' .³¹⁾

$$\epsilon' = \epsilon_{\infty}' \left[1 + \frac{kb}{\sqrt{\pi}} \cdot e^{-b^2 Z_0^2} \int_0^{\infty} e^{-b^2 u^2} \cdot \frac{\cosh(2b^2 Z_0 - 1)u}{\cosh u} \cdot du \right] \quad (27)$$

$$\epsilon'' = \frac{\epsilon_{\infty}' kb}{\sqrt{\pi}} \cdot e^{-b^2 Z_0^2} \int_0^{\infty} e^{-b^2 u^2} \cdot \frac{\cosh 2b^2 Z_0 u}{\cosh u} \cdot du \quad (28)$$

$$Z_0 = \ln \omega \tau_0, \quad u = \ln \omega \tau$$

Assuming the distribution of relaxation times for wood is represented by the probability function, we obtain the following equation for ϵ'' by use of equations (24) and (29).

$$\bar{\phi}(\log \tau) = \frac{n}{\sqrt{2\pi}} \cdot e^{-\frac{n^2 Z^2}{2}} \quad (29)$$

$$\int_{-\infty}^{\infty} \frac{n}{\sqrt{2\pi}} \cdot e^{-\frac{n^2 Z^2}{2}} \cdot dZ = 1$$

$$\log \epsilon'' = \log \left[\frac{\pi(\epsilon_0' - \epsilon_{\infty}')}{4.606} \cdot \frac{n}{\sqrt{2\pi}} \right] - 0.217 n^2 Z^2 \quad (30)$$

$$Z = \log \tau / \tau_0$$

Futhermore, we obtain the equation for ϵ' from equations (25) and (29).

$$\frac{\epsilon' - \epsilon_{\infty}'}{\epsilon_0' - \epsilon_{\infty}'} = \frac{1}{2} + \int_0^x \frac{1}{\sqrt{2\pi}} \cdot e^{-\frac{x^2}{2}} \cdot dx \quad (31)$$

$$x = nZ$$

The value n which represents the width of the distribution of relaxation times is determined by the value ϵ''_{max} .

$$n = \frac{\epsilon''_{max} 4.606 \sqrt{2\pi}}{\pi(\epsilon_0' - \epsilon_{\infty}')} \quad (32)$$

In Figs. 23 and 24 the comparison of the experimental values with the calculated ones for dielectric constant and dielectric loss factor of Hoonoki and western hemlock is shown. The calculated values coincided completely with the experimental ones.

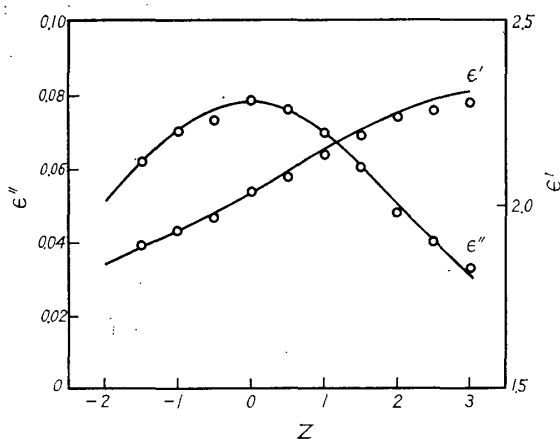


Fig. 23. The comparison of experimental values with calculated values (equations (30) and (31)) for dielectric constant and dielectric loss factor of Hoonoki in L direction at -58°C . O: experimental, -: calculated

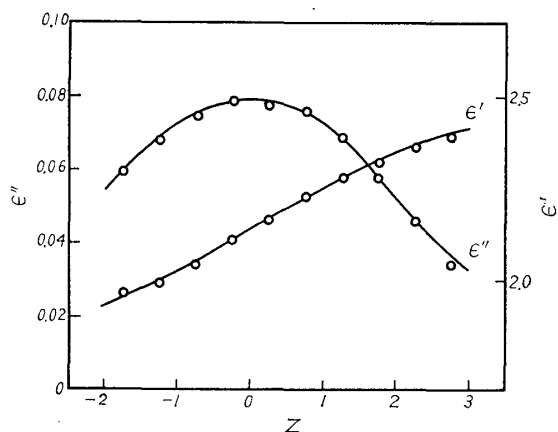


Fig. 24. The comparison of experimental values with calculated values (equations (30) and (31)) for dielectric constant and dielectric loss factor of western hemlock in L direction at -58°C . O: experimental, -: calculated

6. The dielectric anisotropy of wood substance.

By applying the theory of rate process to the dielectric relaxation process, the apparent energy of activation ΔE can be calculated by the following equation.²³⁾

$$\Delta E = -2.303 \cdot R \cdot \frac{d \log f_m}{dT^{-1}} \quad (33)$$

where R , T and f_m are gas constant, absolute temperature and the frequency cor-

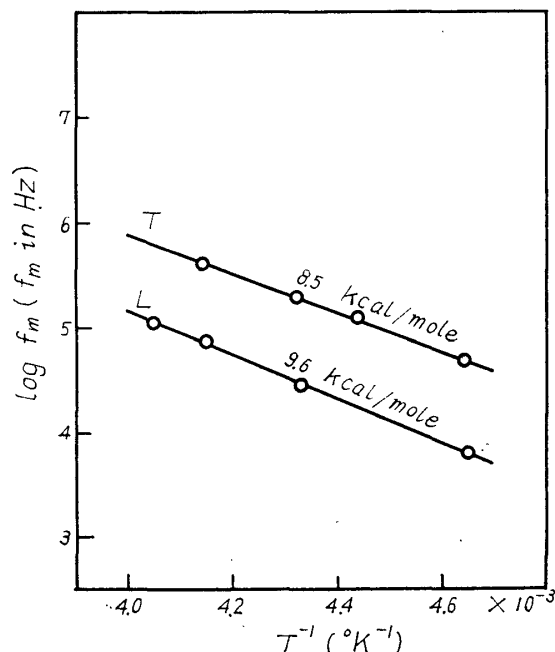


Fig. 25. $\log f_m$ vs. T^{-1} curves for Keyaki in L and T directions.

responding to dielectric loss factor maximum, respectively. In Fig. 25 the curves of f_m versus T^{-1} in L and T directions for Keyaki are shown. The values of ΔE calculated were 9.6 and 8.5 kcal/mole in L and T directions respectively, and the value in L direction was about 1 kcal/mole greater than that in T direction. This result shows that the heights of potential barriers in L direction among the sites are higher than those in T direction and the frequency corresponding to dielectric loss factor maximum in L direction is low by one decade compared with that in T direction. In fact, as shown in Figs. 5, 6 and 7, the frequency corresponding to ϵ''_{max} in L direction was lower than that in the other directions by about one decade.

As previously stated, the value of ϵ' in L direction in low frequency range is greater than that in the other directions. This result shows that the transition probability of dipole jump to an adjacent site when the electric field applies to L direction is considerably greater than that when the electric field applies to the other directions.

References

- 1) KRÖNER, K. und L. PUNGS, Holzforsh., 6, 13 (1952).
- 2) NAKATO, K. and S. KADITÁ, J. Japanese Forestry Soc., 36, 95 (1954).
- 3) UYEMURA, T., Bull. Government Forest Exp. Station, No. 119, 122 (1960).
- 4) SKAAR, C., New York State College of Forestry, Technical Publication, No. 69, 6 (1948).
- 5) NORIMOTO, M. and T. YAMADA, Wood Research, No. 50, 36 (1970).
- 6) LICHTENECKER, K. und K. ROTHER, Phys. Z., 32, 255 (1931).
- 7) WIENER, O., Phys. Z., 5, 332 (1904).
- 8) TAKEMURA, T. and S. MIBAYASHI, Bull. Kyoto Univ. Forests, No. 38, 200 (1966).
- 9) SUZUKI, M. and K. NAKATO, J. Japan Wood Res. Soc., 9, 211 (1963).
- 10) CHRISTENSEN, G. N. and H. F. A. HERGT, Holzforsh, 22, 165 (1968).
- 11) COLE, K. S. and R. H. COLE, J. Chem. Phys., 9, 341 (1941).
- 12) HIGASI, K. et al., J. Phys. Chem., 64, 880 (1960).
- 13) MATSUMOTO, A. and K. HIGASI, J. Chem. Phys., 36, 1776 (1962).
- 14) TAKEDA, M., Kagaku, 18, 21 (1948).
- 15) TSUTSUMI, J., Bull. Kyushu Univ. Forests, No. 41, 109 (1967).
- 16) NANASSY, A. J., Wood Sci. Tech., 4, 104 (1970).
- 17) ISHIDA, Y. et al., J. Appl. Polymer Sci., 1, 227 (1959).
- 18) MIKHAILOV, G. P. et al., Polymer Sci. USSR, 11, 628 (1969).
- 19) ZHBANKOV, R. G., Polymer Sci. USSR, 8, 1962 (1966).
- 20) NORIMOTO, M. and T. YAMADA, Wood Research, No. 46, 1 (1969).
- 21) NORIMOTO, M. and T. YAMADA, J. Japan Wood Res. Soc., 16, 364 (1970).
- 22) DEBYE, P., Polar Molecules, New York, (1929).
- 23) KAUFMANN, W., Rev. Mod. Phys., 14, 12 (1942).
- 24) FRÖHLICH, H., Theory of Dielectrics, Clarendon Press, Oxford, (1958).
- 25) HOFFMAN, J. and H. G. PFEIFFER, J. Chem. Phys., 22, 132 (1954).
- 26) ISHIDA, Y. and K. YAMAFUJI, Kolloid-Z., 177, 97 (1961).
- 27) FUOSS, R. and J. G. KIRKWOOD, J. Am. Chem. Soc., 63, 385 (1941).
- 28) MCCRUM, N. G., B. E. READ and G. WILLIAMS, Anelastic and Dielectric Effects in Polymer

WOOD RESEARCH No. 51 (1970)

- Solids, John Wiley & Sons, London-New York-Sydney, (1967).
- 29) FERRY, J. G., Viscoelastic Properties of Polymer, John Wiley & Sons, New York-London, (1961).
 - 30) WAGNER, K. W., Ann. der Physik, 40, 817 (1913).
 - 31) YAGER, W. A., Physics, 7, 434 (1936).
 - 32) RAFALSKI, J., Holztechnologie, 7, 118 (1966).
 - 33) TRAPP, W. und L. PUNGS, Holzforsch., 10, 65 (1956).